INFN - Laboratori Nazionali di Frascati, May 1995
From: **The Second DaΦne Physics Handbook**[1]
Chapter 9: One Photon Initiated Processes
Eds. L. Maiani, G. Pancheri, N. Paver

Electromagnetic Form Factors

Albert Bramon
Grup de Física Teòrica, Universitat Autònoma de Barcelona,
08193 Bellaterra (Barcelona), Spain
and
Mario Greco
Universita' di Roma III and INFN, Laboratori Nazionali di Frascati,
Frascati, Italy.

Abstract

A general introduction to electromagnetic form factors and hadron production in low-energy e^+e^- machines is discussed. Some global features of existing data are presented and simple, relevant models are briefly commented.

1 Elastic and transition form factors

Low-energy e^+e^--machines are the ideal tool to investigate the time-like region of the electromagnetic form factors (F.F.) of low-mass hadrons, i.e., of the lowest spin mesonic and baryonic states constructed only with u-, d- and s-quarks. The initial e^+e^- pair converts into an exclusive final state containing two particles (A and $\bar{B}$, with four-momenta p and p') through the exchange of a virtual single-photon of squared four-momentum $q^2 = s = (p+p')^2 \geq (m_A+m_B)^2$ as shown in Fig.(1). The amplitude associated to this process is

$$\mathcal{M} = \frac{e^2}{q^2}\bar{v}\gamma^\mu u < A(p)\bar{B}(p') \mid J_\mu^{em} \mid 0 > \qquad (1)$$

where the first factors contain the QED point-like vertex and the photon propagator, whereas the final one, written in terms of the hadronic electromagnetic (e.m.) current

[1]Supported by the INFN, by the EC under the HCM contract number CHRX-CT920026 and by the authors home institutions

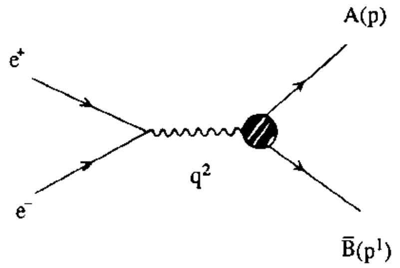

Figure 1: Feynman diagram for $e^+e^- \to \gamma \to A\bar{B}$

and represented by the blob in Fig.(1), incorporates the effects of strong interactions and hadronic structure in one or a few form factors, $F(q^2)$.

From the well-known conservation rules in both strong and e.m. interactions, and the fact that we are exclusively considering processes mediated by a single photon, the two-particle final state is forced to have the photonic quantum numbers too, i.e., $J = 1, P = C = -1$ and isospin $I = 1$ or 0. These quantum numbers can be achieved either with $A = B$ or with $A \neq B$, thus allowing to distinguish between "elastic (or static)" form factors and "transition (or dynamical)" ones, as we now proceed to discuss.

1.1 Elastic Form Factors

If the two hadrons A and B are precisely the same, the final state $A\bar{A}$ has well defined charge conjugation which the above arguments require to be $C = -1$. This immediately implies $F_A(q^2) = -F_{\bar{A}}(q^2)$ and, consequently, the vanishing of the form factors at all q^2 for all the self-conjugate hadrons $A = \bar{A}$, i. e., those having all internal charges equal to zero. This is the case for the truly neutral mesons $\pi^0, \eta, \eta', \rho^0, \omega, \phi, ...$, but not for the electrically neutral mesons K^0, K^{*0} or baryons $n, \Lambda, ...$ having other internal charges and an electromagnetically active substructure.

e^+e^--data for the elastic form factors of a non-neutral hadron A, $F_A(q^2)$, cover the time-like region, $q^2 \geq 4m_A^2$, and complement the values of the corresponding spacelike region, $q^2 \leq 0$. These are deducible from A-elastic scattering experiments on electrons, $eA \to eA$, (as well as on other e.m. fields) and contain the hadronic current matrix element $< A(p) \mid J_\mu^{em} \mid A(p') >$ with $q^2 = t = (p - p')^2 \leq 0$.

1.2 Transition Form Factors

In this case one has a hadron A and two interesting possibilities remain open for the second particle B: it is either another hadron or, alternatively, B is a photon. In the first case, one defines the transition form factors, $F_{AB}(q^2)$, which are non-vanishing for charged A, B hadrons but also for truly neutral ones provided they have opposite charge conjugation. In the second, photonic case, the F.F. $F_A(q^2)$ similarly vanishes except for truly neutral mesons A with positive charge conjugation, i.e., for π^0, η and η', as well as for the poorly known neutral scalars f_0 and a_0.

Again, an e^+e^--machine covers the time-like region of the transition F.F. with $q^2 \geq (m_A + m_B)^2$, but now, if $M_A > m_B$, smaller values of $q^2 \geq 0$ can also be studied using the $A \to Bl^+l^-$ Dalitz decays involving a final lepton pair and requiring $4m_l^2 \leq q^2 \leq (M_A - m_B)^2$. Examples of these processes, for which some knowledge on transition F.F. is already available, are $\omega \to \pi^0\mu^+\mu^-$ and $\eta, \eta' \to \gamma\mu^+\mu^-$.

Space-like values of q^2 can also be explored. One possibility is the use of the so-called Primakoff effect to produce a hadron A through the scattering of a different particle B (which, in particular, can be a real photon) on the virtual photons of the Coulombic field around a nucleus. Again, some data on $\pi\gamma \to \rho, K\gamma \to K^*$ or on $\gamma\gamma \to \pi^0, \eta$ are already known. A second, more powerful possibility consists in investigating the two-photon processes in a conventional e^+e^--machine, $e^+e^- \to e^+e^-M^0$, proceeding through the $\gamma\gamma \to M^0$ subprocess with one or two space-like photon(s) producing a neutral, $C = +1$ meson M^0, such as π^0, η, η', f_0 or a_0.

2 How many independent form factors?

The number of form factors for a given transition is fixed by the number of independent Lorentz structures governing the hadronic matrix element in eq.(1). For a given process, this number, in turn, depends on the number of independent four-vectors at hand (two of them being the A, B four-momentum combinations $p + p'$ and $p - p'$ and, eventually, spin or polarization four-vectors) and the restrictions imposed by Lorentz-invariance, as well as by parity and e.m. charge conservation. The later adopts the form $\partial^\mu J^{em}_\mu = 0$, thus constraining the hadronic matrix element for $e^+e^- \to A\bar{B}$ to satisfy

$$< A(p)\bar{B}(p') \mid J^{em}_\mu \mid 0 > (p + p')^\mu = 0 \tag{2}$$

with $q = (p + p')$ in the time-like region.

Restricting to elastic form factors in the space-like region, the above constraint becomes

$$< A(p') \mid J^{em}_\mu \mid A(p) > (p - p')^\mu = 0 \tag{3}$$

and taking simultaneously into account both the hermiticity of the hadronic current and time-reversal invariance allows for a second, alternative counting and identification of the independent form factors. Moreover, the vanishing of their imaginary part for the whole $q^2 \leq 0$ region is authomatically established via this procedure.

2.1 Elastic F.F. for spinless mesons

This is a particularly relevant case including the pseudoscalar elastic F.F., $F_P(q^2)$, defined as follows

$$< P(p)\bar{P}(p') \mid J_\mu^{em} \mid 0 >= F_P(q^2)(p'-p)_\mu \tag{4}$$

where a second form factor, multiplying the other available four-momentum combination $(p+p')_\mu$, vanishes because of the above charge conservation constraint (2). The normalization is such that $F_P(q^2=0)=\pm 1$, for $P=\pi^\pm, K^\pm$, and $F_P(0)=0$, for $P=K^0, \bar{K}^0$.

Similarly, one expects a single elastic form factor, $F_S(q^2)$, for the up-to-now elusive non-neutral scalar mesons. Transition form factors between a scalar and a pseudoscalar, $F_{PS}(q^2)$, are vanishing because the required axial-vector cannot be constructed with the two independent four-momenta at hand.

2.2 Elastic F.F. for spin 1/2 baryons

In addition to the two independent four-momenta p and p', in this case the four γ-matrices, γ_μ, can be used to construct a third type of vectorial structure, as required by Lorentz invariance. Other combinations of γ-matrices with four-momenta can be easily seen to reduce to the previous three forms using the Dirac equation for the external, on-shell spin 1/2 baryons. On the other hand, as before, current conservation requires the vanishing of a term proportional to $(p+p')_\mu$, thus implying that only two independent form factors are allowed, i.e.,

$$\begin{aligned} < N(p)\bar{N}(p') \mid J_\mu^{em} \mid 0 > &= \bar{u}(p')\{F_1(q^2)\gamma_\mu + \frac{i}{2m_N}\sigma_{\mu\nu}(p+p')^\nu F_2(q^2)\}v(p) \\ &= \bar{u}(p')\{(F_1(q^2)+F_2(q^2))\gamma_\mu + \frac{1}{2m_N}(p-p')_\mu F_2(q^2)\}v(p) \end{aligned} \tag{5}$$

The first line in the previous eq. contains the so-called Dirac and Pauli form factors F_1 and F_2. At $q^2=0$, they are respectively normalized to the electric charge of the baryon N (in units of the proton charge e) and to its anomalous magnetic moment (in units of $e/2m_N$). Their combinations

$$G_E(q^2) = F_1(q^2) + \frac{q^2}{4m_N^2}F_2(q^2), \qquad G_M(q^2) = F_1(q^2) + F_2(q^2) \tag{6}$$

(the latter appearing in the second of eqs.(5) and illustrating the above mentioned reduction procedure via Gordon decomposition of Dirac currents), are the Sachs form factors and verify the interesting property of being equal at the production threshold, $q^2 = 4m_N^2$.

2.3 Transition F.F. for VP and γP

The same arguments as before allow to show the existence of a single form factor for each $\gamma^* \to VP$ or γP transition. Specializing to the $e^+e^- \to V(p^*)P(p)$ case, one has

$$< P(p)V(p^*) \mid J^\mu_{em} \mid 0 >= F_{VP}(q^2)\epsilon^{\mu\nu\alpha\beta}p_\nu\epsilon^*_\alpha p^*_\beta \tag{7}$$

where $F_{VP}(0)$ is normalized to coincide with the VP-coupling constant to real photons governing the well-known $V \to P\gamma$ radiative decay rates. The transition form factor for the γP case has the same characteristics with V replaced by γ and $q^{*2} = 0$. The normalization is now given by the π^0, η and η' couplings to $\gamma\gamma$ and generalization to the case where both photons are off-mass-shell ($q^2, q'^2 \neq 0$) is obvious. In both cases, ϵ^* stands for the final spin-1 polarization and the $\epsilon^{\mu\nu\alpha\beta}$ factor appears because only the pseudoscalar meson belongs to the abnormal spin-parity series.

2.4 Other form factors

A potentially interesting case involves the $e^+e^- \to \gamma S$ reaction, where an elusive neutral scalar S (f_0 or a_0) is produced. Its observation could certainly contribute to solve the old controversy concerning the nature or quark-content of these scalars. The corresponding gauge invariant structure is easily found to be

$$< S(p)\gamma(p*) \mid J_\mu^{em} \mid 0 >= F_{S\gamma}(q^2)\{(\epsilon^* q)p^*_\mu - (p^* q)\epsilon^*_\mu\} \tag{8}$$

For the VS transitions, not restricted now by the gauge invariance of the final photon, two form factors are possible, each one affecting independently one of the two terms in eq.(8).

The number of independent form factors increases when higher spins are considered. Three of them completely describe the e^+e^- production of vector-meson pairs, $V\bar{V}$, such as $\rho^+\rho^-$, $K^*\bar{K}^*$. The situation is kinematically similar to that for the W gauge bosons and suggests the association of the three form factors to the electric charge, dipole magnetic moment and quadrupolar electric moment distributions inside those vector-mesons.

3 Charge radii and slope parameters

As is well known, e.m. form factors of hadrons contain valuable information on their quark structure and, particularly, on the hadronic dimensions or charge distributions. For example, in a non-relativistic potential-theory, assuming an electric charge density $\rho(R)$ inside a hadron, with normalization $\int d^3R\ \rho(R) = 1$, the electrostatic potential produced by a spinless, extended hadron turns out to be

$$V_H(r) = \int d^3R\rho(R)V(\mid \vec{r} - \vec{R} \mid) = F_H(\vec{q}^2)V(\vec{q}^2), \tag{9}$$

where $V(\mid \vec{r} - \vec{R} \mid)$ is the point-like Coulombic potential and the form factor $F_H(\vec{q}^2)$ appears as the Fourier transform of $\rho(R)$

$$F_H(\vec{q}^2) = \int d^3R\ \rho(R)e^{-i\vec{q}\cdot\vec{R}} = 1 - \frac{\vec{q}^2}{6} < r_H^2 > + \dots \tag{10}$$

with $< r_H^2 >= \int d^3RR^2\rho(R)$, known as the mean e.m. squared radius of H, directly connected to its spatial dimensions.

3.1 Charge radii

The essential physical point of the previous discussion can be extended to the case of relativistic field theories and to different form factors. The q^2-dependence of $F_H(q^2)$ is again related to the hadron structure, and mean squared-radii can be defined in anology with eq.(10), i.e.,

$$< r_H^2 >= 6 \left[\frac{dF_H(q^2)}{dq^2} \right]_{q^2=0} \tag{11}$$

A simple example on the relation between these charge radii and the quark substructure in hadrons is clearly offered by the low-mass pseudoscalar mesons consisting of a spinless, s-wave $q\bar{q}$ pair. The squared charge radius of charged pions is known to be about 0.44 fm^2 and can be attributed to the distribution of the (positive) u and $\bar{d}$ constituents of a π^+ around their common CM. In the K^+ case, similarly, the heavier $\bar{s}$ substitutes $\bar{d}$, thus reducing the K^+ dimensions as corroborated by the data (see below). Finally, the negatively charged and light d-quark in a K^0 is worst localized than its positively charged and heavier partner $\bar{s}$ giving therefore rise to the negative K^0 charge radius experimentally measured.

3.2 Slope parameters

To get an idea of the spatial dimensions of (and charge distribution inside) strictly neutral hadrons, one has to extend the above considerations from elastic to transition form factors. Their q^2-slope at $q^2 = 0$, known as the slope parameter b_{AB}, is defined through

$$b_{AB} = \left[\frac{dF_{AB}(q^2)}{dq^2} \right]_{q^2=0} \tag{12}$$

Quite frequently, it is expressed in terms of a parameter Λ_{AB}, having mass-dimensions and verifying $b_{AB} = \Lambda_{AB}^{-2}$. The slope parameter has essentially the same meaning as in the previous case of charge radii, apart from the factor of 6 in the definition.

Slope parameters for the $P\gamma$ transition form factors, with $P = \pi^0, \eta$ and η', have been measured (Λ_P in the $0.75 - 0.81$ GeV range or, equivalently, $6b_P$ in the $0.43 - 0.36$ fm^2 range) indicating that their dimensions are quite compatible (once one accounts for the factor of 6) with those previously discussed for their SU(3)-partners. In both cases, one measures the spatial region where the electromagnetically active hadron constituents can be found. In the first, charge-radius case one has to deal with electrostatic or Coulombic interactions, while, in the later $\gamma P \to \gamma$ transitions, magnetic interactions are involved with quark-spin flipping and $q\bar{q} \to \gamma$ annihilations.

4 Pseudoscalar form factors

The differential cross-section for $e^+e^- \to P\bar{P}$ can be deduced from eqs.(1,2) and written in terms of the single pseudoscalar form factor. In the CM-system, one has

$$\frac{d\sigma}{d\Omega} = \frac{\alpha^2}{8s} \mid F_P(s) \mid^2 \sin^2\theta(1 - 4m_P^2/s)^{3/2} \tag{13}$$

for $s = q^2 \geq 4m_P^2$ and $P = \pi^+,\ K^+$ or K^0.

4.1 Pion form factor

The pion form factor has been measured in a rather wide range of q^2-values as shown in Fig.(2). The time-like region, $q^2 \geq 4m_\pi^2$, has been accurately explored by various e^+e^--machines not only in the interesting region around the ρ, ω, ϕ resonances, where F_π and $\sigma(e^+e^- \to \pi^+\pi^-)$ are large, but also at much higher q^2-values. Experimental details and references can be seen in the reviews by Bauer et al [1] and Dolinsky et al [2]. The reaction $\pi^-p \to e^+e^-n$ (inverse electroproduction), on the other hand, allows to cover the lower q^2-region just above $4m_e^2$.

For q^2-values in the space-like region, good data are also available (most of them from elastic $e\pi$ scattering, but also from the (π-electroproduction) reaction $eN \to e\pi N$; see ref. [3], for details). Some of them are also shown in Fig.(2).

All the gross features of these data are approximately explained by a simple ρ-meson Breit-Wigner dominating this pion form factor. This reasonable simple-pole description clearly suggests and illustrates the success of naive vector-meson dominance models (VMD). Interesting modifications to this simple one-pole behaviour have been detected around the ω and ϕ peaks, showing again the relevance of vector-mesons even in isospin violating channels. Other structures seem to be present at higher energies as discussed in ref. [4]. At asymptotic energies, the Brodsky-Farrar quark counting rules, derived from QCD, predict the simple pole dependence $F_P(Q^2) \to 1/Q^2$ [5].

From the well measured behaviour around $q^2 = 0$, the pion charge radius can be defined. We quote the value

$$< r_{\pi^+}^2 >= 0.44 \ \pm \ 0.03 \ fm^2 \tag{14}$$

coming essentially from ref.[6] but coinciding with several independent measurements and their global mean value [7] with one exception: that coming from old data [8] on $e\pi \to e\pi$ and leading to $< r_{\pi^+}^2 >= 0.31 \ \pm \ 0.03 \ fm^2$.

As far as Daphne is concerned, a high precision measurement of the pion form factor near the threshold, as well as in the region around the ρ-meson, is crucial for reducing the theoretical error in the hadronic contribution to the muon anomalous magnetic moment (see Franzini's contribution to this chapter). Similarly, Daphne offers exceptional opportunities to improve the measurements of $F_\pi(q^2)$ around the ϕ-peak. This is essential to understand the $u\bar{u}, d\bar{d}$ contaminations in the mainly $s\bar{s}$ ϕ-meson wave function.

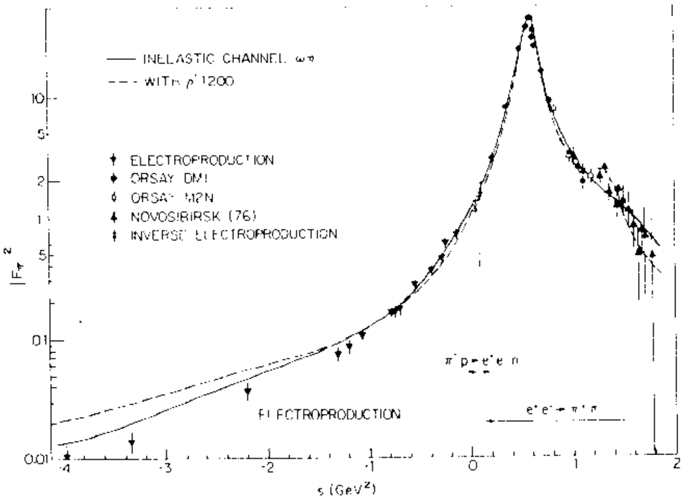

Figure 2: A plot of the pion form factor versus energy as determined from colliding beams, inverse electroproduction and electroproduction measurements. Details and fits can be found in ref.[1]

4.2 Kaon F.F.

The threshold for kaon pair production in e^+e^--machines is just below the ϕ-peak. Therefore, the quite good data already available for $F_{K^+,K^0}(q^2)$ should be considerably improved in Daphne. They follow, as expected, the ϕ Breit-Wigner excitation curve, as schematically shown in Figs.(3) and (4). Some data for higher q^2-values are also existing above the ϕ-peak, where F_{K^+} is found to be larger than F_{K^0} (see Figs.(5) and (6)). Further details can be seen in the compilations [1] and [2], as well as in their references to original work.

A few determinations of the kaon charge radii are also available. They lead to [10]

$$< r^2_{K^+} >= 0.31 \ \pm \ 0.05 \ fm^2 \qquad < r^2_{K^0} >= -0.054 \ \pm \ 0.026 \ fm^2 \tag{15}$$

and to the difference [6] $< r^2_{\pi^+} > - < r^2_{K^+} >= 0.13 \ \pm \ 0.04 \ fm^2$, as qualitatively discussed when dealing with the physical meaning of these charge-radii.

The vector part of the K_{l3} decays gives further information on the related $K\pi$ transition form factor. Indeed, from the PDG compilation one deduces [11]

$$< r^2_{K\pi} >= 0.36 \ \pm \ 0.02 \ fm^2 \tag{16}$$

while Sirlin's theorem [9], which is valid up to first order in SU(3) breaking, predicts $2 < r^2_{K\pi} > - 2 < r^2_{K^0} >=< r^2_{\pi^+} > + < r^2_{K^+} >$. The good agreement with the above values adds some confidence to the whole set of data and their interpretation.

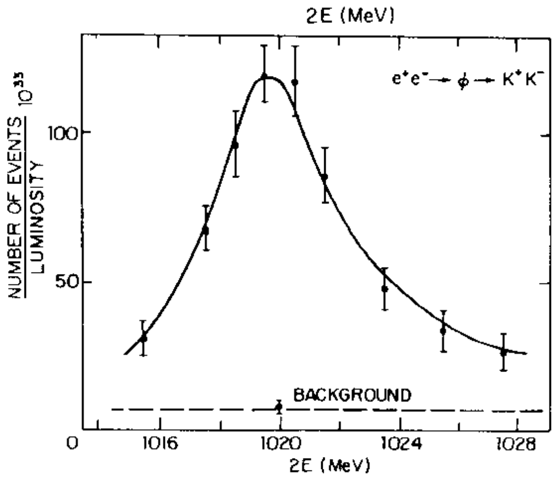

Figure 3: Exitation curves for the ϕ resonance decaying into K^+K^-.

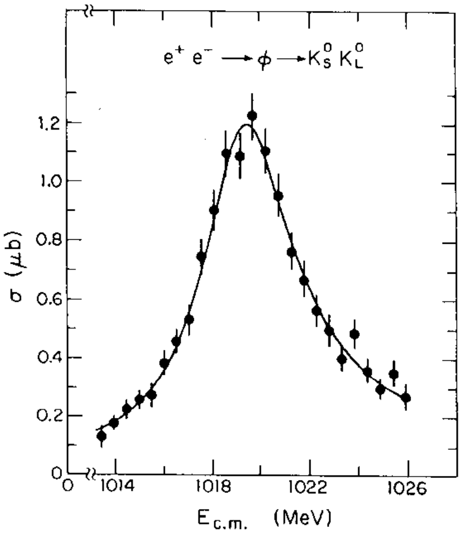

Figure 4: Cross-section for $e^+e^- \rightarrow \phi \rightarrow K_S^0 K_L^0$.

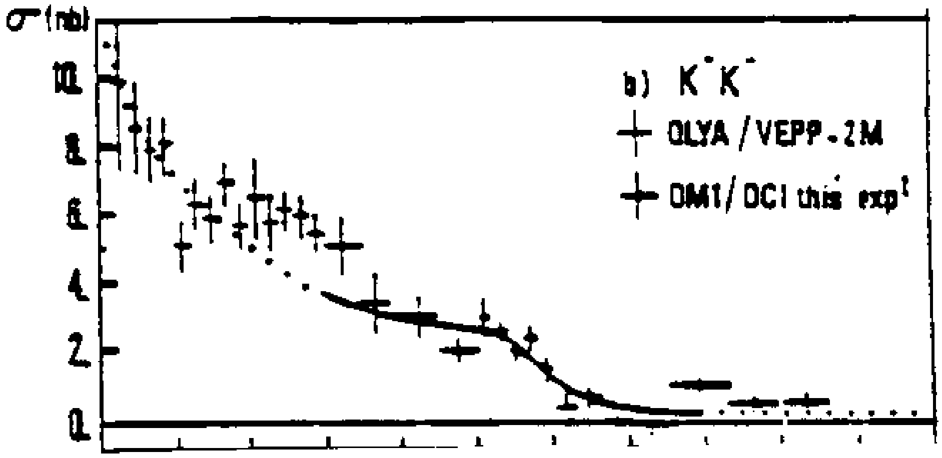

Figure 5: The K^+ e.m. form factor as a function of energy.

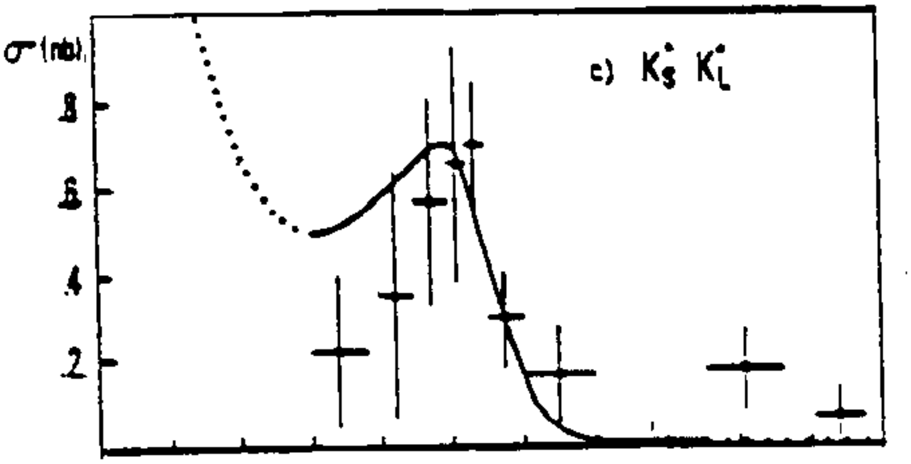

Figure 6: The K^0 e.m. form factor as a function of energy.

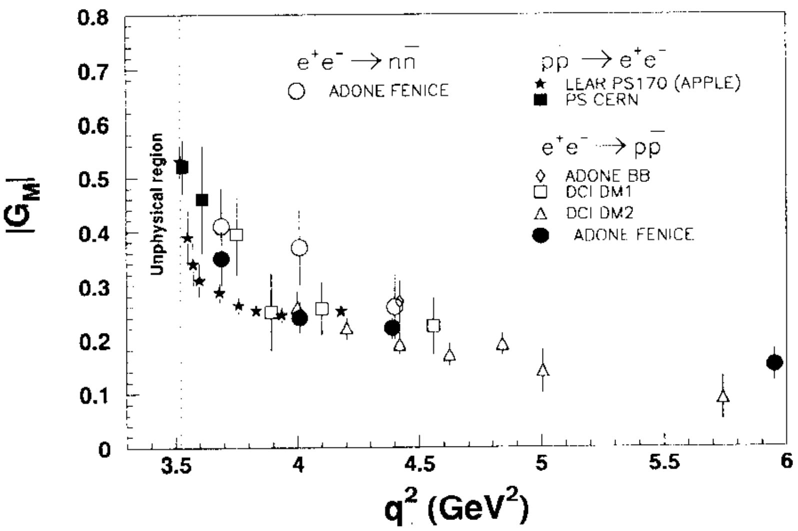

Figure 7: The proton and neutron e.m. form factors as a function of $s^{1/2}$.

5 Nucleon form factors

The CM differential cross-section for $e^+e^- \to N\bar{N}$ is most conveniently expressed in terms of the Sachs form factors as

$$\frac{d\sigma}{d\Omega} = \frac{\alpha^2 m_N^2}{s}\left((1+\cos^2\theta)(s/4m_N^2) \mid G_M(s) \mid^2 + \sin^2\theta \mid G_E(s) \mid^2\right)(1-4m_N^2/s)^{1/2} \quad (17)$$

From this eq. and working above threshold, proton, neutron and other baryon form factors can, in principle, be extracted in an e^+e^--machine. However, being far from the narrow resonance region, the cross-section is rather low and statitistics is hard to collect. Assuming the above mentioned equality of magnetic and electric Sachs form factors at threshold, early measurements have given information with large errors. Recently, more precise data have been produced and also the neutron form factor has been measured for the first time. These results are shown in Fig.(7)

On the other hand, one has excellent data from elastic eN-scattering for $q^2 \leq 0$. Here, both the F_1 and F_2 (or G_E and G_M) form factors can be separately measured for both protons and neutrons, as well as for their isoscalar or isovector combinations. We don't discuss these results explicitly, being only of secondary interest for Daphne, but simply recall that a reasonable description of these data can be achieved by a "universal" dipole fit

$$G_E^p(q^2) = G_M^p(q^2)/\mu_p = G_M^n(q^2)/\mu_n = G_D(q^2) = \left(1 - q^2/(0.71GeV)^2\right)^{-2} \quad (18)$$

for $q^2 \leq 0$.

The corresponding electric and magnetic charge radii are found to be in the range of $0.77 - 0.92\ fm$, i.e., only moderately above the charge radii for charged pseudoscalars. Further details and references for nucleon form factors can be found in refs. [3] and [12]. Concerning the asymptotic behaviour expected from the quark counting rules [5], it coincides with the dipole formula $F_N(Q^2) \to (1/Q^2)^2$.

6 γP and VP transition form factors

The CM integrated cross-section for $e^+e^- \to VP$ or γP can be simply expressed in terms of the single relevant transition form factor as

$$\sigma(q^2 = s) = \frac{4\pi\alpha^2}{3s^{3/2}} \mid F_{VP,\gamma P}(s) \mid^2 \mid \vec{p}_P \mid^3 \tag{19}$$

where the form factors, $F_{VP}(s)$ or $F_{\gamma P}(s)$, have been normalized as in eq.(7) and $\vec{p}_P$ is the final CM momentum.

6.1 VP transition F.F.

The paradigmatic example of VP transition form factors is $F_{\omega\pi}(q^2)$, which has been explored above the $\omega\pi$-threshold through e^+e^--annihilation and, quite independently, in the $4m_\mu^2 \leq q^2 \leq (m_\omega - m_\pi)^2$ interval through the Dalitz decay $\omega \to \pi^0\mu^+\mu^-$. The global set of experimental data, taken from ref. [13], are displayed in Fig.(8) . Again, a simple ρ-meson Breit-Wigner gives a rough description of the data in the two separate regions, below and above the ρ-peak. The slope parameter $b_{\omega\pi} = \Lambda_{\omega\pi}^{-2}$ has been measured to correspond to $\Lambda_{\omega\pi} = 0.65 \pm 0.03\ GeV$, somewhat below the ρ-mass. Of course the data in the higher mass region give possible evidence for excited ρ states. The situation is discussed in detail by Donnachie and Clegg [14]. Daphne is expected to play a major role in clarifying the whole matter.

The SU(3) rotated version of the above transition $\phi \to \eta\mu^+\mu^-$ should be observed by Daphne and, if higher energies are reachable, its crossed version $e^+e^- \to \phi\eta$ could be studied too. Comparison with the $\omega\pi$ case could be of interest when studying SU(3)-breaking in this sector.

6.2 γP transition F.F.

e^+e^--machines have been already used to obtain some information on the $\gamma\pi$ and $\gamma\eta$ transition form factors around the ρ, ω, ϕ peaks, where the cross-section is large and interference effects are of interest. Some results can be seen in refs. [2] and [11] and play a central role in identifying the precise quark content of the above vector-mesons.

However, the corresponding slope parameters are more accurately known through the (virtual) gamma-gamma scattering processes in e^+e^- reactions. Indeed, the data coming

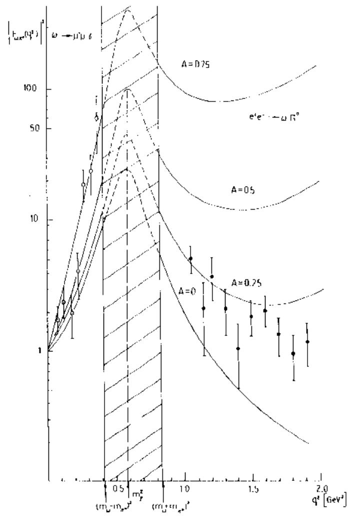

Figure 8: Study of the transition form factor in $\omega \to \pi^0 \mu^+ \mu^-$ decay and in the reaction $e^+e^- \to \omega\pi^0$. Details can be found in ref.[13].

from different teams are in nice agreement and may be averaged to give (see ref. [16] for details)

$$\Lambda_{\pi^0} = 0.75 \pm 0.03\ GeV, \quad \Lambda_\eta = 0.77 \pm 0.04\ GeV \quad \Lambda_{\eta'} = 0.81 \pm 0.04\ GeV \tag{20}$$

Asymptotically, one expects [5] $F_{\gamma P} \to 1/Q^2$ and the related Brodsky-Lepage interpolation formula [17] predicts $\Lambda_\pi = 2\pi f_\pi = 0.83\ GeV$, not far from (20).

7 Models for form factors

Our present understanding of the strong interactions governing quark dynamics is based on the QCD lagrangian from which no reliable information can be extracted except for asymptotic Q^2-values. In this region, quark counting rule predictions can be deduced as we have already briefly discussed. In the remaining q^2-regions, accessible to low-energy e^+e^- machines, no valid theoretical predictions are available and several phenomenological models have been proposed. Examples are the Vector Meson Dominance (VMD) model (where the similarities between vector-mesons and photons are exploited) and constituent quark models with their underlying SU(3) symmetry (where the hadronic constituents are phenomenologically taken into account). Q^2- or QCD-duality [18] can be invoked to link these two approaches, but for theoretically more justified points of view one has to rely on the Chiral Perturbation Theory (ChPT) approach to pseudoscalar charge radii [15] and [19].

7.1 VMD for q^2 near the resonance region

A general review on VMD and many of its results can be found in ref. [1]. Here, we simply concentrate on the main formulae for e^+e^- annihilations. In this case, the crucial point in the model is the assumption that the blob in Fig.(1), connecting the intermediate photon to the final hadronic state, reduces to a vector meson (or sum over vector mesons) propagator(s). More precisely, the diagram is assumed to contain a γV conversion vertex (with a coupling given by em_V^2/f_V), followed by the V-propagator and the final V-decay vertex into f (with a g_{Vf} coupling constant). The cross-section turns out to be

$$\sigma_{e^+e^-\to V\to f}(s) = \frac{4\pi\alpha^2 F(s)}{3s^{3/2}} \mid \sum_V A_V \mid^2 \tag{21}$$

with the sum extending over the relevant V-mesons, F(s) being the final phase space factor and

$$A_V = \frac{g_{Vf}}{f_V}\frac{m_V^2}{m_V^2 - s - im_V\Gamma_V(s)}. \tag{22}$$

The values of the f_V couplings can be extracted from e^+e^- data [11] through $\Gamma(V \to e^+e^-) = 4\pi\alpha^2 m_V/3f_V^2$ and are essentially compatible with the nonet symmetry and ideal $\omega-\phi$ mixing predictions $f_\rho = f_\omega/3 = -\sqrt{2}f_\phi/3$. For the various final states f, one has $\Gamma(V \to f) = g_{Vf}^2 F(s)/12\pi$ in such a way that the e^+e^--cross section factorizes into a V-production and V-decay factor. More explicitly, at a resonance peak, one has

$$\sigma_{e^+e^-\to V\to f}(s = m_V^2) = 12\pi\Gamma(V \to e^+e^-)\Gamma(V \to f)/m_V^2\Gamma_V^2 \tag{23}$$

The particularization of the above formulae to the pseudoscalar form factor case is extremely simple. For pions one has

$$F_{\pi^+}(s) = \frac{m_\rho^2}{m_\rho^2 - s - im_\rho\Gamma_\rho(s)} \equiv BW_\rho(s), \tag{24}$$

where the VMD relation $f_\rho = g_{\rho\pi\pi}$ has been used. For kaons one similarly obtains

$$\begin{aligned} F_{K^+}(s) &= +\frac{1}{2}BW_\rho(s) + \frac{1}{6}BW_\omega(s) + \frac{1}{3}BW_\phi(s), \\ F_{K^0}(s) &= -\frac{1}{2}BW_\rho(s) + \frac{1}{6}BW_\omega(s) + \frac{1}{3}BW_\phi(s) \end{aligned} \tag{25}$$

where the numerical coefficients follow from SU(3) Clebsch-Gordans and quark charges. These F.F. satisfy the simple VMD relation $F_\pi(s) + F_{K^0}(s) = F_{K^+}(s)$.

The above simple equations give a quite reasonable description of pseudoscalar pair production below 1.5 GeV, thus showing the adequacy of the naive VMD hypothesis. For a more accurate description further details and fine tuning of parameters is required. This proceeds in two main directions. One consists in extending the sum not only to the lowest-lying V-mesons but also to their high-mass recurrencies or radial excitations. Small improvements are then obtained along the lines of refs. [18] [4] and [14]. A second line of improvement consists in introducing SU(3)-breaking effects as described in detail in a next section [15]. The later are of interest in Daphne, where $\omega - \phi$ and $\rho - \phi$ mixings (or, equivalently, the precise quark content of the ϕ) should be accurately measured.

The $P\gamma$ transition form factors are readily obtained in the VMD context. Now one has

$$F_{P\gamma}(s) = \sum_V \frac{g_{VP\gamma}}{f_V} \frac{m_V^2}{m_V^2 - s - i m_V \Gamma_V(s)} \tag{26}$$

leading to an economical and reasonable description of the data. Again, some improvements can be performed along the same lines as before. Details can be found in refs. [16] and [15] in these proceedings.

7.2 Models for F.F. near $q^2 = 0$ and charge radii

Far from resonance peaks, the role played by V-mesons can be reproduced by other dynamical mechanisms. This is the case for charge radii and their related slope parameters, both defined around $q^2 = 0$. In VMD, the previously discussed expressions for $F_P(s)$ lead to simple formulae and reasonable values for the pseudoscalar charge radii

$$< r^2_{\pi^+} >= 6/m_\rho^2 = 0.39\ fm^2, \quad < r^2_{K^+} >= 0.36\ fm^2, \quad < r^2_{K^0} >= -0.03\ fm^2. \tag{27}$$

These values satisfy the VMD-relation $< r^2_{K^+} > - < r^2_{\pi^+} >=< r^2_{K^0} >$ but are only in rough agreement with data (eqs.(14) and (15)). The situation can easily be improved, as discussed in ref. [15], and extended to the transition F.F. and their slope parameters (b and Λ). In all these cases (the K^0 case is somehow exceptional, as we already discussed), the V-meson mass fixes correctly the scale with m_V near Λ.

But constituent-quark model ideas can also be useful in this field. A simple quark-loop gives finite predictions for charge radii, which are quite close to those from VMD provided the quark mass is fixed to $m_q^2 = m_V^2/12$, near the constituent quark-mass value (see, ref. [16] for details and related work). SU(3)-breaking can similarly be introduced through the $m_s - m_{u,d}$ mass difference. Further reasonable predictions are also known for the slope parameters [16] thus supporting the general idea of Q^2- or QCD-duality, i.e., that VMD (or mesonic) contributions and (fermionic) quark-loop effects are somehow dual or equivalent and, in particular, cannot be added [18].

ChPT is, however, the more valid and QCD inspired approach to account for the pseudoscalar charge radii. The K^0 charge radius is unambiguously predicted to be $-0.036\ fm^2$ near experiment. For charged pions and kaons one obtains reasonable values and the VMD-like relation $< r^2_{K^+} > - < r^2_{\pi^+} > = < r^2_{K^0} >$. Improvements and further details can be found in ref. [15] in these proceedings.

References

[1] T.H.Bauer et al. Rev. Mod. Phys. 50 (1978) 261.

[2] S.I.Dolinsky et al. Phys. Rep. $\underline{C202}$ (1991) 99.

[3] M.M.Nagels et al. Nucl. Phys. $\underline{B147}$ (1979) 189.

[4] S.Dubnicka, Nuov. Cim. $\underline{100A}$ (1988) 1;
M.E.Biagini et al., Nuov. Cim. $\underline{104A}$ (1991) 363.

[5] S.J.Brodsky and J.R.Farrar, Phys. Rev. $\underline{D11}$ (1975) 1309.

[6] E.B.Dally et al. Phys. Rev. Lett. $\underline{48}$ (1982) 375.

[7] P.Gensini, Phys. Rev. $\underline{D17}$ (1978) 1368.

[8] E.B.Dally et al. Phys. Rev. Lett. $\underline{39}$ (1977) 1176.

[9] A. Sirlin, Phys. Rev. Lett. $\underline{43}$ (1979) 904.

[10] S.R.Amendolia et al. Phys. Lett. $\underline{B178}$ (1986) 435;
W.R.Molzon et al. Phys. Rev. Lett. $\underline{41}$ (1978) 1231.

[11] Particle Data Group. Phys. Rev. $\underline{45}$ (1992) S1.

[12] B.Bartoli et al., Riv. Nuov. Cim. $\underline{2}$ (1972) 241.

[13] L.G.Landsberg Phys. Rep. $\underline{C128}$ (1985) 301 and references therein.

[14] A. Donnachie and A.B.Clegg, these proceedings.

[15] A.Bramon, A.Grau and G.Pancheri, these proceedings.

[16] Ll.Ametller et al. Phys. Rev. $\underline{D45}$ (1992) 986 and references therein.

[17] S.J.Brodsky and G.P.Lepage, Phys. Rev. $\underline{D24}$ (1981) 1808.

[18] A. Bramon, E. Etim and M. Greco, Phys. Lett. $\underline{41B}$ (1972) 609;
M. Greco, Nucl. Phys. $\underline{B63}$ (1973) 398.

[19] J.Gasser et al. in these Proceedings.